Quantizer Design for Distributed GLRT Detection of Weak Signal in Wireless Sensor Networks

Fei Gao, Lili Guo, *Member, IEEE*, Hongbin Li, *Senior Member, IEEE*, Jun Liu, *Member, IEEE*, and Jun Fang, *Member, IEEE*

***Abstract*—We consider the problem of distributed detection of a mean parameter corrupted by Gaussian noise in wireless sensor networks, where a large number of sensor nodes jointly detect the presence of a weak unknown signal. To circumvent power/bandwidth constraints, a multilevel quantizer is employed in each sensor to quantize the original observation. The quantized data are transmitted through binary symmetric channels to a fusion center where a generalized likelihood ratio test (GLRT) detector is employed to perform a global decision. The asymptotic performance analysis of the multibit GLRT detector is provided, showing that the detection probability is monotonically increasing with respect to the Fisher information (FI) of the unknown signal parameter. We propose a quantizer design approach by maximizing the FI with respect to the quantization thresholds. Since the FI is a nonlinear and nonconvex function of the quantization thresholds, we employ the particle swarm optimization algorithm for FI maximization. Numerical results demonstrate that with 2- or 3-bit quantization, the GLRT detector can provide detection performance very close to that of the unquantized GLRT detector, which uses the original observations without quantization.**

***Index Terms*—Wireless sensor networks, multilevel quantization, distributed detection, particle swarm optimization algorithm (PSOA).**

I. Introduction

WIRELESS sensor networks (WSNs) have attracted considerable interest over the past decades (see [1]–[8], and references therein), due to the reliability, flexibility, cost-effectiveness and ease of deployment. A WSN may consist of a large number of spatially distributed sensors linked with a fusion center (FC). The constituting sensors can be employed to provide measurements of a given physical process (temperature, humidity, etc.) as well as to detect specific events (mobile target, alarms, etc.) over a region of interest [9]. Distributed detection is a fundamental problem in WSNs, on which extensive studies have been conducted [10]–[14].

Due to stringent power/bandwidth constraints, each sensor may be required to quantize its observations, before transmitting its data to the FC where a global decision is performed [7], [8], [15], [16]. The simplest and coarsest quantizer is the one-bit quantizer consisting of a single threshold. This one-bit quantization significantly reduces the communication burden from the sensor to the FC, but at the expenses of some performance loss. Specifically, one-bit quantizer design for distributed detection is considered in [17], where a generalized likelihood ratio test (GLRT) detector is employed at the FC. Asymptotic performance analysis of the one-bit GLRT detector is provided for cases where the quantized data are transmitted to the FC via perfect or imperfect channels. In [18], a one-bit Rao detector is proposed as a computationally efficient alternative to the one-bit GLRT detector. There is a notable performance gap between the one-bit detector and the unquantized detector without quantization [17]. This is because a considerable amount of useful information is lost when the original observations are quantized into only one-bit data. Clearly, one expects that the performance gap can be closed by resorting to multilevel quantizers, and it is of interest to examine the design of multilevel quantizers for distributed detection.

Multilevel quantization for distributed detection and estimation has been investigated in a multitude of studies [8], [19]–[28]. The main challenge is the high computational complexity as the design of a multilevel quantizer often involves a nonlinear multi-dimensional search process [11]. In [19], a multilevel quantizer is employed in an automatic digital radar detector to quantize the radar video in amplitude and range. The quantization thresholds are determined using an empirical procedure to avoid exhaustive search. In [20], a quasi-optimum multilevel quantizer is obtained with a gradient algorithm to maximize the detection probability which can be approximately expressed as a function of quantization thresholds. However, the gradient algorithm is time-consuming and computationally prohibitive when the number of quantization levels is large. In addition, it is not guaranteed to converge to the optimum quantization levels. A suboptimum multilevel quantization scheme with improved computational efficiency is proposed by using fuzzy techniques in [23]. Nevertheless, as stated in [23], the disadvantage of this method is that it is generally unknown how to map the local likelihood ratio to a fuzzy set to provide the best detection performance for different scenarios. The authors in [24] consider

Manuscript received May 20, 2014; revised September 28, 2014; accepted December 1, 2014. Date of publication December 8, 2014; date of current version April 7, 2015. This work was supported in part by the U.S. National Science Foundation under Grant ECCS-1408182 and in part by the National Science Foundation of China under Grant 61428103. The associate editor coordinating the review of this paper and approving it for publication was C. Tepedelenlioglu.

F. Gao and L. Guo are with the College of Information and Communication Engineering, Harbin Engineering University, Harbin 150001, China (e-mail: feigao.1208@gmail.com; guolili@hrbeu.edu.cn).

H. Li is with the Department of Electrical and Computer Engineering, Stevens Institute of Technology, Hoboken, NJ 07030 USA (e-mail: hongbin.li@stevens.edu).

J. Liu is with the National Laboratory of Radar Signal Processing, Xidian University, Xi'an 710071, China (e-mail: junliu@xidian.edu.cn).

J. Fang is with the National Key Laboratory of Science and Technology on Communications, University of Electronic Science and Technology of China, Chengdu 611731, China (e-mail: junfang@uestc.edu.cn).

Color versions of one or more of the figures in this paper are available online at http://ieeexplore.ieee.org.

Digital Object Identifier 10.1109/TWC.2014.2379279

the distributed detection problem with multilevel quantization in each local sensor. However, the multilevel quantizer is constrained to be uniform in [24], i.e., the quantization thresholds are constrained to be equally spaced. The GLRT fusion rule based on soft decision is introduced in [26] where the target is jointly detected and localized with improved performance compared with a counting rule. Notice that in all above investigations on multilevel quantization for distributed detection and estimation, the communication channel from the sensors to the FC center is assumed to be error-free. In practice, this channel is in general prone to noise, and hence the quantized data may be subjective to distortion during the transmission to the FC. A cooperative spectrum sensing structure was investigated in [29], where local M-level quantized data are reported through distortion channels and fused at the FC. The erroneous channels were molded based on quantization output values.

In this work, we are mainly concerned on the design of multilevel quantizers for distributed detection of a weak signal [12], [30]. Specifically, the problem is to detect a mean parameter corrupted by Gaussian noise in a WSN where the channels from the local sensors and the FC may be imperfect. We first quantize the original observations into multi-bit data. These quantized data are coded into binary codewords, and are then transmitted to the FC through distortion channels modeled as binary symmetric channels (BSCs). Using the quantized data received at the FC, we propose a GLRT detector to make a global decision about the presence or absence of an unknown signal. An asymptotic performance analysis based on a weak-signal assumption of this GLRT detector is provided, revealing that the quantization thresholds play an important role in the detection performance. More specifically, the detection probability is monotonic with respect to the unknown signal's Fisher information (FI). Given this insight, we propose a quantizer design approach by maximizing the FI with respect to the quantization thresholds. Since the objective function (i.e., the FI) is nonlinear and non-convex in the quantization thresholds, for which a gradient search is not effective, we resort to a particle swarm optimization algorithm (PSOA) [31] to search for the thresholds corresponding to the maximum FI. The PSOA is a stochastic global optimization method modeled after social behavior such as bird flocking and fish schooling [32]. It does not require any gradient information on the objective function, and as well is easy to implemented.

Simulation results show that the detector proposed here with multilevel quantization significantly outperforms the one-bit detector proposed in [17]. More importantly, it is demonstrated that, the GLRT detector using 2- or 3-bit quantized data can provide detection performance very close to the unquantized detector which has full access to the original unquantized sensor observations. Hence, through suitable quantizer design, each sensor only needs to send 2 or 3 bits of information per measurement, which is adequate to achieve the unquantized detection performance, and further increase in the quantization level does not bring in an obvious gain in the detection performance.

The rest of the paper is organized as follows: In Section II, we formulate the distributed detection problem with multi-bit quantization. In Section III, a multi-bit GLRT scheme is proposed. In Section IV, we present an asymptotic analysis of the multi-bit GLRT detector, and design the multilevel quantizers by using the PSOA. Numerical results and comparisons are provided in Section V. Finally, concluding remarks are given in Section VI.

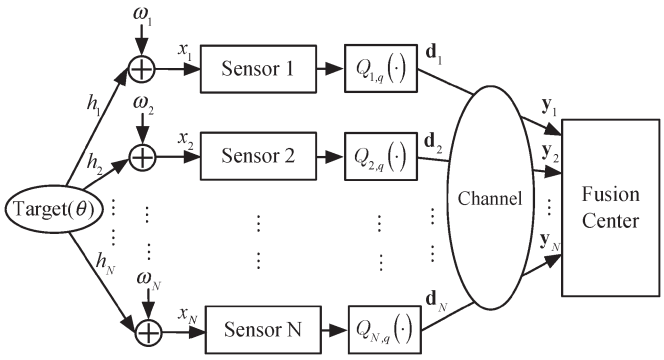

Fig. 1. A distributed detection system.

Notation: Vectors (matrices) are denoted by boldface lower (upper) case letters, all vectors are column vectors; superscript $(\cdot)^T$ denotes transposition; $E\{\cdot\}$ represents statistical expectation; $\mathbb{Z}^+$ symbolizes a set of positive integers; $\mathbb{R}^n$ signifies the n-dimensional space of real numbers; $[\tau_1,\tau_2]^n$ represents an n-dimensional space, where each dimension is limited to $[\tau_1,\tau_2]$; $\|\cdot\|$ is the Euclidean norm of a vector.

II. Problem Formulation

Consider the problem of distributed detection of an unknown scalar deterministic signal parameterized by θ in the presence of zero-mean additive white Gaussian noise (AWGN), as depicted in Fig. 1. Assume that there are N spatially distributed sensors, and each sensor obtains a noisy observation of θ. Let the null hypothesis (H_0) be that the observations are signal free and the alternative hypothesis (H_1) be that the observations contain a signal. The detection problem based on all the observations can be formulated as the following binary hypothesis testing:

$$\begin{aligned} H_0 &: x_n = w_n \\ H_1 &: x_n = h_n\theta + w_n, \quad n = 1,2,\ldots,N, \end{aligned} \tag{1}$$

where the subscript n is the sensor index; x_n denotes the nth sensor's observation; $h_n \in \mathbb{R}$ are the known observation coefficients defining the input/output relation of the nth sensor [17], [18]; w_n represents the AWGN with zero mean and known variance $\sigma^2_{w_n}$. The noise at the local sensors is assumed to be independent across the sensors.

To circumvent stringent bandwidth/energy limitations, we have to quantize the sensors' observations before transmitting them to the fusion center (FC). Assume that a q-bit quantizer denoted by $Q_{n,q}$ $(q \in \mathbb{Z}^+)$ is employed in the nth sensor where the observation is compared with a set of quantization thresholds $\{\tau_{n,k}\}_{k=0}^{2^q}$ with $\tau_{n,0} = -\infty, \tau_{n,2^q} = +\infty$. The output of $Q_{n,q}$, indicating which interval the observation lies in, is encoded as a binary codeword denoted by $\mathbf{d}_n \in \{0,1\}^q$ before being transmitted to the FC over binary symmetric channels (BSCs). Relying on the received data $\mathbf{y}_n$, the FC forms a global decision

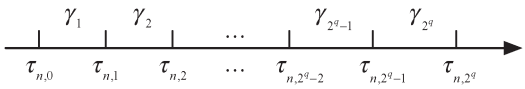

Fig. 2. q-bit quantizer.

regarding the presence or absence of the signal θ. Obviously, the quantization level and the quantization thresholds play a vital role in this detection problem. The problem of interest here is to design the q-bit quantizer in each sensor to assist detecting the signal θ in the FC.

III. GLRT-Based Fusion Rule

In this section, we assume the quantization thresholds $\{\tau_{n,k}\}_{k=0}^{2^q}$ are predetermined for each sensor, and we derive a generalized likelihood ratio test (GLRT) based fusion rule at the FC to detect θ from distorted data $\{\mathbf{y}_n\}_{n=1}^{N}$. Quantizer design will be considered in the next section. Before deriving the GLRT rule, we briefly discuss q-bit quantization and the distortion channel to introduce necessary notation.

A. q-Bit Quantizer

Fig. 2 shows the quantization characteristics for the q-bit quantizer $Q_{n,q}$ at the nth sensor. Each q-bit quantizer $Q_{n,q}$ involves a set of ordered thresholds $\{\tau_{n,k}\}_{k=0}^{2^q}$ with $\tau_{n,0} = -\infty, \tau_{n,2^q} = +\infty$. Note that the threshold sets of the quantizers for different sensors are not constrained to be the same.

For fixed n and q, the real line $\mathbb{R}$ is demarcated by thresholds $\{\tau_{n,k}\}_{k=0}^{2^q}$ into 2^q non-overlapping quantization intervals. Each quantization interval is uniquely labeled using a label set $\Gamma = \{\gamma_1, \gamma_2, \ldots, \gamma_{2^q}\}$. Each label γ_i can be encoded as a q-bit binary codewords $\mathbf{b}_{n,i} = [b_{n,i,q}, b_{n,i,q-1}, \ldots, b_{n,i,1}]^T$, where $b_{n,i,j} \in \{0,1\}$. Hence, the output codeword of the q-bit quantizer at the nth sensor can be expressed as

$$\mathbf{d}_n = \begin{cases} \mathbf{b}_{n,1}, & \infty < x_n < \tau_{n,1}, \\ \mathbf{b}_{n,2}, & \tau_{n,1} \le x_n < \tau_{n,2}, \\ \vdots & \vdots \\ \mathbf{b}_{n,2^q}, & \tau_{n,2^q-1} \le x_n < +\infty, \end{cases} \tag{2}$$

where x_n and $\mathbf{d}_n$ are the input and output of the q-bit quantizer at nth sensor, respectively.

Denote by $P_{w_n}^{n,j}(\theta)$ the probability that the observation x_n at the nth sensor falls into the jth quantization interval $[\tau_{n,j-1}, \tau_{n,j})$. Then, under hypothesis H_1, we have

$$\begin{aligned} P_{w_n}^{n,j}(\theta) &= P(\mathbf{d}_n = \mathbf{b}_{n,j}; \theta) \\ &= P(\tau_{n,j-1} \le x_n < \tau_{n,j}; \theta) \\ &= F_{w_n}(\tau_{n,j-1} - h_n\theta) - F_{w_n}(\tau_{n,j} - h_n\theta), \end{aligned} \tag{3}$$

where $F_{w_n}(\cdot)$ is the complementary cumulative density function (CCDF) of the Gaussian noise w_n.

B. Distortion Channel: BSC

Assume that the distortion channels from all sensor nodes to the FC are independent, and each of them can be modeled with a BSC as illustrated in Fig. 3, where $\tilde{P}$ is the crossover probability, and $1-\tilde{P}$ is the probability of correctly receiving 0 or 1. Suppose further that each bit can be independently transmitted over the BSC.

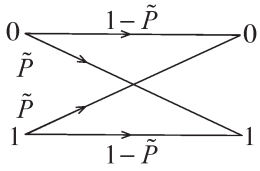

Fig. 3. Binary symmetric channel (BSC) model.

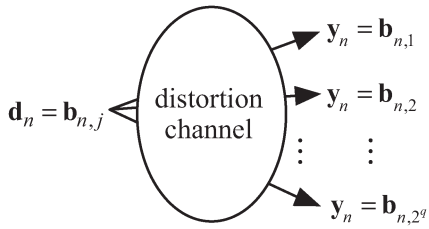

Fig. 4. The distortion channel from the nth sensor to the FC.

Fig. 4 shows the output of the BSC with the input $\mathbf{d}_n = \mathbf{b}_{n,j}$ $(1 \le j \le 2^q)$. Due to the distortion effect in the BSC, the output $\mathbf{y}_n$ may potentially be any one of the binary codewords. The probability that $\mathbf{b}_{n,j}$ is changed to $\mathbf{b}_{n,i}$ over the BSC can be calculated as

$$\begin{aligned} &P(\mathbf{y}_n = \mathbf{b}_{n,i} | \mathbf{d}_n = \mathbf{b}_{n,j}) \\ &\quad = \tilde{P}^{D_{n,i,j}} (1-\tilde{P})^{(q - D_{n,i,j})} \\ &\quad = G(q, \tilde{P}, D_{n,i,j}), \end{aligned} \tag{4}$$

where $D_{n,i,j}$ is the Hamming distance between $\mathbf{b}_{n,i}$ and $\mathbf{b}_{n,j}$ defined as

$$D_{n,i,j} \triangleq D(\mathbf{b}_{n,i}, \mathbf{b}_{n,j}) = q - \sum_{k=0}^{q-1} I(b_{n,i,q-k}, b_{n,j,q-k}), \tag{5}$$

with the indicator function $I(\cdot)$ being

$$I(A,B) = \begin{cases} 1, & A = B, \\ 0, & \text{otherwise.} \end{cases} \tag{6}$$

Note that the Hamming distance $D_{n,i,j}$ is the total of incorrectly received bits for each transmitted received codeword pair between $\mathbf{b}_{n,i}$ and $\mathbf{b}_{n,j}$.

The probability mass function (PMF) of the output $\mathbf{y}_n$ of the BSC under H_1 is given by

$$\begin{aligned} P(\mathbf{y}_n; \theta) &= \sum_{i=1}^{2^q} \sum_{j=1}^{2^q} P(\mathbf{y}_n = \mathbf{b}_{n,i} | \mathbf{d}_n = \mathbf{b}_{n,j}) P(\mathbf{d}_n = \mathbf{b}_{n,j}) \\ &= \prod_{i=1}^{2^q} \left\{ \sum_{j=1}^{2^q} G\left(q, \tilde{P}, D_{n,i,j}\right) P_{w_n}^{n,j}(\theta) \right\}^{I(\mathbf{y}_n, \mathbf{b}_{n,i})}, \end{aligned} \tag{7}$$

where $P(\mathbf{d}_n = \mathbf{b}_{n,j})$ is defined in (3) and we note in the second equality, the indicator function $I(\mathbf{y}_n, \mathbf{b}_{n,i})$ is zero except for one specific i when it equals 1 (i.e., when $\mathbf{y}_n$ takes that codeword $\mathbf{b}_{n,i}$).

C. GLRT Detector

Due to the unknown parameter θ, we resort to the GLRT [33] to solve the detection problem in (1). The GLRT detector can be obtained by replacing the unknown parameter with its maximum likelihood (ML) estimate, i.e.,

$$T_q(\mathbf{Y}) = \frac{P(\mathbf{Y};\hat{\theta},H_1)}{P(\mathbf{Y};H_0)} \underset{H_0}{\overset{H_1}{\gtrless}} \eta, \tag{8}$$

where the subscript q means that the test statistic is for the case of the q-bit quantization scheme; η is a detection threshold; $\mathbf{Y} = [\mathbf{y}_1, \mathbf{y}_2, \ldots, \mathbf{y}_N]$ is the input data matrix of the FC; $P(\mathbf{Y};\hat{\theta},H_1)$ and $P(\mathbf{Y};H_0)$ denote the PMFs or likelihood function of $\mathbf{Y}$ under H_1 and H_0, respectively; $\hat{\theta}$ is the ML estimate under H_1.

Specifically, the likelihood function under H_1 is given by

$$\begin{aligned} &P(\mathbf{Y};\theta,H_1) \\ &= \prod_{n=1}^{N} P(\mathbf{y}_n;\theta) \\ &= \prod_{n=1}^{N}\prod_{i=1}^{2^q} \left\{ \sum_{j=1}^{2^q} G\left(q,\tilde{P},D_{n,i,j}\right) P_{w_n}^{n,j}(\theta) \right\}^{I(\mathbf{y}_n,\mathbf{b}_{n,i})}. \end{aligned} \tag{9}$$

We can obtain $\hat{\theta}$ by

$$\hat{\theta} = \arg\max_{\theta} \left[P(\mathbf{Y};\theta,H_1)\right], \tag{10}$$

whereas $P(\mathbf{Y};H_0)$ can be obtained from $P(\mathbf{Y};\theta,H_1)$ by setting $\theta = 0$. In general, the ML estimate of θ rarely admits a closed-form expression. However, it can be verified that $P(\mathbf{Y};\theta,H_1)$ is a concave function for Gaussian noise [34]. Therefore, any one-dimensional gradient-based search starting from a random initial estimate is guaranteed to converge to the global maximum, and many efficient routines exist for this type of work [35]. Substituting the ML estimate $\hat{\theta}$ in (8), we can obtain the final GLRT detector.

IV. Quantizer Design

In this section, we first provide an asymptotic performance of the GLRT detector, which leads to design criterion for the optimization of the q-bit quantizers. Next, we discuss how to use the particle swarm optimization algorithm (PSOA) to solve the optimization problem.

A. Asymptotic Performance Analysis

According to [33], the asymptotic statistical distribution of the modified test statistic, i.e., $2\ln T_q(\mathbf{y})$, is[1]

$$2\ln T_q(\mathbf{Y}) \overset{a}{\sim} \begin{cases} \chi_1^2, & \text{under } H_0, \\ \chi_1'^2(\lambda_q), & \text{under } H_1, \end{cases} \tag{11}$$

[1]Equation (11) holds under the weak signal condition, i.e., θ is relatively small compared to the noise variance. For most WSN applications, it is weak signal detection that is of primary interest. If the signal to be detected is strong, a few sensors along with a standard quantization schemes (e.g., uniform quantizer) would suffice.

where "a" denotes an asymptotic distribution; χ_r^2 denotes a Chi-squared distribution with r degrees of freedom (DOFs); $\chi_r'^2(\lambda_q)$ designates a non-central Chi-squared distribution with r DOFs and the non-centrality parameter λ_q. Moreover, the non-centrality parameter λ_q is expressed as

$$\lambda_q = (\theta_1 - \theta_0)^2 \mathcal{F}_q(\theta_0), \tag{12}$$

where $\theta_0 = 0$ and $\theta_1 = \theta$ is the value of θ under H_1; $\mathcal{F}_q(\theta)$ represents the Fisher information (FI) given by (see Appendix A for details)

$$\mathcal{F}_q(\theta) = \sum_{n=1}^{N} h_n^2 \sum_{i=1}^{2^q} \frac{\left\{\sum_{j=1}^{2^q} G\left(q,\tilde{P},D_{n,i,j}\right) \rho_{w_n}^{n,j}(\theta)\right\}^2}{\sum_{j=1}^{2^q} G\left(q,\tilde{P},D_{n,i,j}\right) P_{w_n}^{n,j}(\theta)}, \tag{13}$$

where

$$\rho_{w_n}^{n,j}(\theta) = p_{w_n}(\tau_{n,j-1} - h_n\theta) - p_{w_n}(\tau_{n,j} - h_n\theta), \tag{14}$$

and $p_{w_n}(\cdot)$ denotes the probability density function (PDF) of the observation noise w_n. The Cramér-Rao bound (CRB) for θ is given by

$$\mathrm{CRB}_\theta = \frac{1}{\mathcal{F}_q(\theta)}. \tag{15}$$

B. Design Criterion of q-Bit Quantizers

We can see from (11) that the larger the non-centrality parameter λ_q, the better the detection performance. Notice that the non-centrality parameter λ_q given in (12) is a monotonically increasing function with respect to the FI evaluated in $\theta = \theta_0$ which is associated with the $(2^q - 1)$-dimensional quantization threshold vectors $\boldsymbol{\tau}_n \overset{\Delta}{=} [\tau_{n,1}, \tau_{n,2}, \ldots, \tau_{n,2^q-1}]$, $n = 1, 2, \ldots, N$. It is worth remarking that $\tau_{n,0} = -\infty$ and $\tau_{n,2^q} = +\infty$ for arbitrary n. The two extreme thresholds are no longer included in the threshold sets which are to be examined.

The best asymptotic detection performance of the GLRT detector can be achieved by solving the following optimization problem:

$$\max_{\{\tau_n\}_{n=1}^N} \sum_{n=1}^{N} h_n^2 \sum_{i=1}^{2^q} \frac{\left\{\sum_{j=1}^{2^q} G(q,\tilde{P},D_{n,i,j}) \rho_{w_n}^{n,j}(0)\right\}^2}{\sum_{j=1}^{2^q} G(q,\tilde{P},D_{n,i,j}) P_{w_n}^{n,j}(0)}. \tag{16}$$

For convenience of mathematical computation, the noise distribution is normalized to have a unit variance: $\tilde{w}_n = w_n/\sigma_{w_n} \sim \mathcal{N}(0,1)$. Thus, the optimization problem is recast to

$$\max_{\{\tau_n\}_{n=1}^N} \sum_{n=1}^{N} \frac{h_n^2}{\sigma_{w_n}^2} \sum_{i=1}^{2^q} \frac{\left\{\sum_{j=1}^{2^q} G\left(q,\tilde{P},D_{n,i,j}\right) \rho_{\tilde{w}_n}^{n,j}(0)\right\}^2}{\sum_{j=1}^{2^q} G\left(q,\tilde{P},D_{n,i,j}\right) P_{\tilde{w}_n}^{n,j}(0)}, \tag{17}$$

where

$$\rho_{\tilde{w}_n}^{n,j}(0) = p_{\tilde{w}_n}\left(\frac{\tau_{n,j-1}}{\sigma_{w_n}}\right) - p_{\tilde{w}_n}\left(\frac{\tau_{n,j}}{\sigma_{w_n}}\right), \tag{18}$$

$$P_{\tilde{w}_n}^{n,j}(0) = F_{\tilde{w}_n}\left(\frac{\tau_{n,j-1}}{\sigma_{w_n}}\right) - F_{\tilde{w}_n}\left(\frac{\tau_{n,j}}{\sigma_{w_n}}\right), \tag{19}$$

with $p_{\tilde{w}_n}$ and $F_{\tilde{w}_n}$ denoting the PDF and CCDF of $\tilde{w}_n$, respectively.

Because of the previous assumption that the distortion channels are independent, the above optimization equation decouples into N independent optimization problems:

$$\max_{\boldsymbol{\tau}_n} \quad g_n(\boldsymbol{\tau}_n), \tag{20}$$

where

$$g_n(\tau_n) = \sum_{i=1}^{2^q} \frac{\left\{\sum_{j=1}^{2^q} G\left(q,\tilde{P},D_{n,i,j}\right)\rho_{\tilde{w}_n}^{n,j}(0)\right\}^2}{\sum_{j=1}^{2^q} G\left(q,\tilde{P},D_{n,i,j}\right)P_{\tilde{w}_n}^{n,j}(0)}, \tag{21}$$

where we omit the constant $\frac{h_n^2}{\sigma_{\tilde{w}_n}^2}$ in each objective function. For ease of notation, we drop the index n and rewrite (20) as

$$\begin{aligned} &\max_{\boldsymbol{\tau}} g(\boldsymbol{\tau}) \\ &\text{s.t. } \boldsymbol{\tau} = [\tau_1,\tau_2,\ldots,\tau_{2^q-1}]^T, \\ &\qquad -\infty < \tau_1 < \tau_2 < \ldots < \tau_{2^q-1} < +\infty, \end{aligned} \tag{22}$$

where the order constraint on the thresholds is explicitly imposed.

An intuitive discussion on the decoupling of the quantization threshold is in order. In distributed detection involving an unknown parameter with a finite range, it is common that a set of different thresholds is employed by different sensors nodes so that a better detection performance would be achieved, because some of thresholds are potentially close to the unknown parameter. However, in this paper, the unknown deterministic parameter is assumed to be weak ($\theta \approx 0$), and thus all thresholds tend to be identical. Conventional optimization methods such as the gradient search method (GSM) [36, p. 34], to a great extent, rely on the assumption of the cost function's characteristics (e.g., concavity, convexity, and monotonicity). Such optimization methods are not suitable to the above optimization problem, since the cost function g in (22) exhibits, non-linear and non-convex properties. In the following, we resort to the particle swarm optimization algorithm (PSOA) to search the solution to the optimization problem in (22).

C. PSOA-Based Solution

The PSOA proposed first by Kennedy and Eberhart [37] is a stochastic optimization method inspired by the social cooperative and competitive behaviors of bird flocking and fish schooling. It has been successfully applied to address many high-dimensional, non-convex optimization problems [38]. The PSOA is initialized with a swarm of candidate solutions (called particles) randomly positioned in a high dimensional search space. Each particle has two primary operators: velocity update and position update. During each iteration, the velocity and position of each particle is dynamically adjusted according to its personal best position and the global best position found by the entire swarm so far.

Applying the PSOA to (22), we assume that a swarm of M particles explore the (2^q-1)-dimensional hyperspace Δ in search of a solution. Assume that the search interval for each dimension of Δ is restricted to $[-\tau_{\max},\tau_{\max}]$, where $\tau_{\max}$ denotes the maximum position limitation. At the end of this subsection, we will discuss the selection of Δ. The ith particle $(i = 1,2,\ldots,M)$ at the kth iteration is described by two characteristics: position vector $\boldsymbol{\tau}_i^k = [\tau_{i,1}^k,\tau_{i,2}^k,\ldots,\tau_{i,2^q-1}^k]$ and velocity vector $\mathbf{v}_i^k = [v_{i,1}^k, v_{i,2}^k,\ldots,v_{i,2^q-1}^k]$.

We set the current iteration counter $k = 0$ and independently initialize $\tau_{i,j}^0$ according to a uniform distribution on $[-\tau_{\max},\tau_{\max}]$. In order to prevent the particles from leaving the search space Δ, we initialize $v_{i,k}^0$ according to a uniform distribution in $[-v_{\max},v_{\max}]$ (as in, e.g., [32, p. 39]), where $v_{\max} = [\tau_{\max} - (-\tau_{\max})]/2 = \tau_{\max}$. For the order constraint in (22), the mechanism for confining $\tau_{i,j}$ is described as follows:

$$\text{If } \tau_{i,j-1}^k > \tau_{i,j}^k, \text{ then set } \tau_{i,j-1}^k = \tau_{i,j}^k - \varepsilon, 2 \le j \le 2^q - 1; \tag{23}$$

where ε is an arbitrary small positive real number. Based on the initial particles $\{\boldsymbol{\tau}_i^0\}_{i=1}^M$, we set the initial personal best position $\boldsymbol{pbest}_i^0$ of the ith particle to be

$$\boldsymbol{pbest}_i^0 = \boldsymbol{\tau}_i^0,\ i = 1,2,\ldots,M. \tag{24}$$

Substituting the initial particles $\{\boldsymbol{\tau}_i^0\}_{i=1}^M$ into the objective function $g(\cdot)$ in (22), we obtain a set of values $\{g(\boldsymbol{\tau}_i^0)\}_{i=1}^M$, and then set the initial global best position $\boldsymbol{gbest}^0$ to be

$$\boldsymbol{gbest}^0 = \arg\max_{\{\boldsymbol{\tau}_i^0\}} \{g\left(\boldsymbol{\tau}_1^0\right), g\left(\boldsymbol{\tau}_2^0\right),\ldots,g\left(\boldsymbol{\tau}_M^0\right)\}. \tag{25}$$

At the $(k+1)$st iteration, the velocity vector $\mathbf{v}_i^{k+1}$ and position vector $\boldsymbol{\tau}_i^{k+1}$ of the ith particle is updated as, respectively,

$$\mathbf{v}_i^{k+1} = K\left[\mathbf{v}_i^k + c_1 r_{i,1}^k\left(\boldsymbol{pbest}_i^k - \boldsymbol{\tau}_i^k\right) + c_2 r_{i,2}^k\left(\boldsymbol{gbest}^k - \boldsymbol{\tau}_i^k\right)\right] \tag{26}$$

and

$$\boldsymbol{\tau}_i^{k+1} = \boldsymbol{\tau}_i^k + \mathbf{v}_i^{k+1}, \tag{27}$$

where $r_{i,1}^k$ and $r_{i,2}^k$ are random numbers uniformly distributed within [0,1]; the positive constants c_1 and c_2 represent the acceleration coefficients that guide the particles towards the personal best and global best positions, respectively; K is a constriction factor given by [31]

$$K = \frac{2}{\left|2 - \varphi - \sqrt{\varphi^2 - 4\varphi}\right|}, \tag{28}$$

with $\varphi = c_1 + c_2$ and $\varphi > 4$. Usually, these two constants c_1 and c_2 are assigned to be 2.05 [31]. Inserting them into (28) yielding $K = 0.7298$.

Denote by $\boldsymbol{pbest}_i^k = [pbest_{i,1}^k, pbest_{i,2}^k,\ldots,pbest_{i,2^q-1}^k]$ the personal best position achieved by the ith particle at the kth iteration. The update criterion for the position of the ith particle at the $(k+1)$ iteration is given by

$$\boldsymbol{pbest}_i^{k+1} = \begin{cases} \boldsymbol{pbest}_i^k, & \text{if } g\left(\boldsymbol{\tau}_i^{k+1}\right) \le g\left(\boldsymbol{pbest}_i^k\right), \\ \boldsymbol{\tau}_i^{k+1}, & \text{if } g\left(\boldsymbol{\tau}_i^{k+1}\right) > g\left(\boldsymbol{pbest}_i^k\right). \end{cases} \tag{29}$$

The global best position $\boldsymbol{gbest}^{k+1}$ at the $(k+1)$st iteration is obtained by comparing all the personal best positions updated

by particles until the kth iteration, namely,

$$\boldsymbol{gbest}^{k+1} = \arg \max_{\{\boldsymbol{pbest}_i^{k+1}\}} \left\{ g\left(\boldsymbol{pbest}_1^{k+1}\right), \cdots, g\left(\boldsymbol{pbest}_M^{k+1}\right) \right\}. \quad (30)$$

Notice that it is possible for some particles to move outside $[-\tau_{max}, \tau_{max}]^{2^q-1}$ during the iteration process. To avoid this, we impose the following step in iterations [32, p. 41], [38]:

$$\begin{aligned} &\text{If } \tau_{i,j}^{k+1} > \tau_{max}, \text{ then } \tau_{i,j}^{k+1} = \tau_{max}; \\ &\text{else if } \tau_{i,j}^{k+1} < -\tau_{max}, \text{ then } \tau_{i,j}^{k+1} = -\tau_{max}. \end{aligned} \quad (31)$$

The above steps are repeated until a termination criterion is met. Here, we stop the termination when the following condition is satisfied [39]

$$\left\| \mathbf{v}_i^k \right\| \leq v_{tol}, \quad (32)$$

where v_{tol} denotes the stopping tolerance velocity.

Finally, the whole iterative optimization procedures are summarized in Algorithm 1.

Algorithm 1 PSOA for Quantizer Optimization

Input: v_{tol}, v_{max}, τ_{max}, c_1, c_2, $r_{i,1}^0$, $r_{i,2}^0$, K, M, N, q
Output: a solution $\boldsymbol{\tau}^\star$ to (22)

1) Set $k := 0$, randomly initialize $\boldsymbol{\tau}_i^0 \in [-\tau_{\max}, \tau_{\max}]^{2^q-1}$ and $\mathbf{v}_i^0 \in [-v_{\max}, v_{\max}]^{2^q-1}$ for $1 \leq i \leq M$;
2) Alter the initial position $\boldsymbol{\tau}_i^0$ by (23);
3) Evaluate $g(\boldsymbol{\tau}_i^0)$, and set $\boldsymbol{pbest}_i^0$ and $\boldsymbol{gbest}^0$ by (24) and (25), respectively;
4) Update the velocity $\mathbf{v}_i^{k+1}$ and the position $\boldsymbol{\tau}_i^{k+1}$ by (26) and (27), respectively;
5) Alter the position $\boldsymbol{\tau}_i^{k+1}$ by (23) and (31);
6) Evaluate $g(\boldsymbol{\tau}_i^{k+1})$ for $1 \leq i \leq M$, and update $\boldsymbol{pbest}_i^{k+1}$ and $\boldsymbol{gbest}^{k+1}$ by (29) and (30), respectively;
7) Set $k := k+1$;
8) Repeat Step 4–Step 7 until $\|\mathbf{v}_i^{k+1}\| \leq v_{tol}$;

Output: $\boldsymbol{\tau}^\star = \boldsymbol{gbest}^{k+1}$.

We now discuss the choice of the search space Δ. There are two main reasons why each dimension of the search space Δ is constrained in a finite interval $[-\tau_{max}, \tau_{max}]$. First, each parameter to be examined in (22) corresponds to a threshold which affects the objective function $g(\cdot)$ through the CCDF of a normal Gaussian variable. It is well known that the normal Gaussian distribution is mainly concentrated on a finite interval. Second, the restriction on the search space is often imposed in the PSOA algorithm [32, p. 41], which can significantly alleviate the computational burdens.

V. Numerical Results

In this section, numerical simulations are conducted to illustrate the performance of the proposed quantization and detection techniques. In the simulations, we assume $h_n = 1$ and $\sigma_{w_n}^2 = 1$ for all n. In addition, we select $\theta = 0.5$, $P_{FA} = 0.1$, $M = 100$, $\tau_{\max} = 5$, and $v_{tol} = 10^{-6}$.

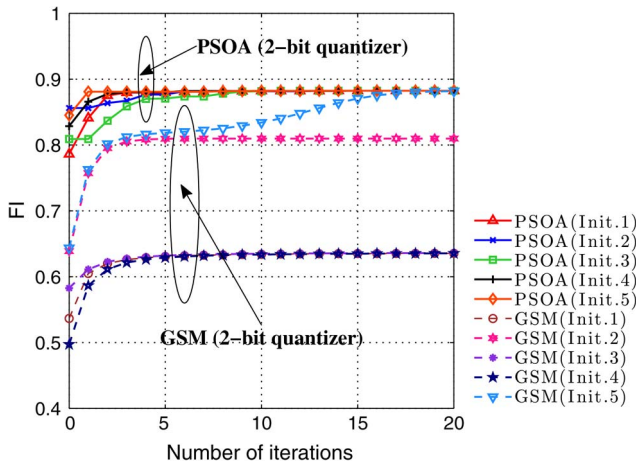

Fig. 5. Comparisons between the convergence behaviors of the PSOA and the GSM for different initializations.

TABLE I
Comparison of the CPU Time of the PSO and GSM in the Error-Free Channels (Unit: Seconds)

Scheme	2-bit		3-bit	
Algorithm	PSO	GSM	PSO	GSM
Run-time	1.980	1.466	8.129	7.964

A. PSOA Versus GSM

Fig. 5 compares the FI values obtained by using the PSOA and the conventional GSM for $q = 2$. For each search algorithm, we use five different random initializations. Each initialization for the GSM is independently and uniformly drawn from the search space Δ. It is noted that each initialization for the PSOA is obtained with (25). Specifically, first we independently draw M points (i.e., particles) from the search space Δ, and then use the global best position as the initialization. Inspections of Fig. 5 highlight that the largest FI is consistently obtained by using the PSOA with different initializations, while the GSM is not guaranteed to obtain the largest value of FI, and may converge to local maxima with different initializations. Table I shows that the comparison of the CPU time incurred by the PSO and GSM algorithms for the 2-bit and 3-bit cases in error-free channels. The runtime of the PSO based approach is slightly longer than that of the GSM counterpart because of the larger number of function evaluations required by PSO.

B. Quantizer Design

We now examine the quantization thresholds obtained by using the PSOA. As an example, we consider the cases of $q = 2$ and 3. The optimum quantization thresholds obtained by using the PSOA for $q = 2$ and 3 are reported in Tables II and III, respectively. We consider five different crossover probabilities, i.e., $\tilde{P} = 0, 10^{-3}, 10^{-2}, 10^{-1}, 0.2$. In particular, $\tilde{P} = 0$ corresponds to the channel without distortion.

From Tables II and III, it is observed that each set of thresholds for the q-bit quantizer is symmetric with respect to the middle threshold $\tau = 0$. This can be explained by two facts. First, is that the Gaussian distribution of the noise is symmetric;

TABLE II
2-BIT QUANTIZER FOR DIFFERENT $\tilde{P}$

thresholds \ $\tilde{P}$	0	10^{-3}	10^{-2}	10^{-1}	0.2
$\tau_0^\star$	$-\infty$	$-\infty$	$-\infty$	$-\infty$	$-\infty$
$\tau_1^\star$	-0.9816	-0.9689	-0.8750	-0.4458	-0.2384
$\tau_2^\star$	0	0	0	0	0
$\tau_3^\star$	0.9816	0.9689	0.8750	0.4458	0.2384
$\tau_4^\star$	$+\infty$	$+\infty$	$+\infty$	$+\infty$	$+\infty$
$g(\boldsymbol{\tau}^\star)$	0.8825	0.8776	0.8369	0.5661	0.3542

TABLE III
3-BIT QUANTIZER FOR DIFFERENT $\tilde{P}$

thresholds \ $\tilde{P}$	0	10^{-3}	10^{-2}	10^{-1}	0.2
$\tau_0^\star$	$-\infty$	$-\infty$	$-\infty$	$-\infty$	$-\infty$
$\tau_1^\star$	-1.7479	-1.6788	-1.3756	-4.9999	-4.9999
$\tau_2^\star$	-1.0500	-1.0002	-0.7485	-4.9991	-4.9991
$\tau_3^\star$	-0.5005	-0.4747	-0.3262	-0.5683	-0.3152
$\tau_4^\star$	0	0	0	0	0
$\tau_5^\star$	0.5005	0.4747	0.3262	0.5683	0.3152
$\tau_6^\star$	1.0500	1.0002	0.7485	4.9991	4.9991
$\tau_7^\star$	1.7479	1.6788	1.3756	4.9999	4.9999
$\tau_8^\star$	$+\infty$	$+\infty$	$+\infty$	$+\infty$	$+\infty$
$g(\boldsymbol{\tau}^\star)$	0.9655	0.9588	0.9119	0.6424	0.4405

Second, the noise PDF is unimodal around zero. We note that the latter fact does not always guarantee threshold-symmetry around zero, even in the single-bit case, when other noise PDFs are employed (e.g. the generalized Gaussian distribution), as shown in [40]. Although our algorithm can be used to design quantizers for noise with an arbitrary distribution, we consider only the case of Gaussian noise in our simulation.

Using these quantization thresholds in Tables II and III, we can obtain that the non-centrality parameters λ_q for $q = 2$ and 3 in the case of the errorless channel are, respectively,

$$\lambda_2 \approx 0.8825\lambda_\infty, \tag{33}$$

and

$$\lambda_3 \approx 0.9655\lambda_\infty. \tag{34}$$

where $\lambda_\infty \stackrel{\Delta}{=} \theta^2 \sum_{n=1}^{N} \frac{h_n^2}{\sigma_{w_n}^2}$ represents the non-centrality of the unquantized case. Apparently, relative to the unquantized case, $q = 3$ entails a smaller loss than $q = 2$. This explains why the 3-bit GLRT detector outperforms the 2-bit one.

It is worth noting that the optimum quantization thresholds for $\tilde{P} = 0$ in Tables II and III are the same as those obtained in [41]. Nevertheless, our method is different from that in [41]. First, the criteria of designing the optimum quantizer are distinct. Our criterion here is to maximize the detection performance of the GLRT fusion scheme, while the criterion in [41] is to retain as much signal fidelity as possible to reconstruct the signal at the receiver. Second, the search algorithms used in [41] and our work are different.

For the purpose of comparison, we have included the uniform quantizer in some of the simulation results. The 1-bit uniform quantizer is the same as our 1-bit quantizer with $\tau = 0$. We have added uniform quantizer for 2-bit and 3-bit cases whose dynamic ranges are [−5,5] with 4 and 8 levels, respectively. Some discussions of the choice of the uniform quantizers are in order. On the one hand, for the uniform quantizer, we have to set the dynamic range of the signal to be quantized. For our detection problem, the dynamic range is unknown under H_1, since θ is unknown. So in practice, there is some difficulty of using the uniform quantizer. On the other hand, the performance of the uniform quantizer is quite sensitive when the dynamic range used for the uniform quantizer is either too small or too large. Our choice of [−5,5] for the considered simulation set-ups represents a better scenario for the uniform quantizer. Therefore, the corresponding quantization thresholds are [−2.5, 0, 2.5] for 2-bit quantizer, and [−3.75, −2.5, −1.25, 0, 1.25, 2.5, 3.75] for 3-bit quantizer.

Next, the performance of the ML estimator for the unknown parameter θ is examined. The MSEs of the estimators for θ are presented using Monte Carlo (MC) techniques for different quantization bits in Fig. 6. The quantization thresholds are obtained by using the PSOA. The number of MC trials for each case is 10^5. For comparison purposes, the CRB of the estimator for θ is also provided by using (15). As shown in [42, p. 30], the CRB for the unquantized approach without quantization is $\mathrm{CRB}_{\mathrm{NQ}}(\theta) = \sigma^2/N$, where the subscript NQ represents no quantization. Note that the unquantized approach provides a lower performance bound, since it has full access to the sensors' original observations without any quantization loss.

It is shown in Fig. 6(a) that when the channel is error-free (i.e., $\tilde{P} = 0$), the MSE is consistent with the corresponding CRB in each quantization case. In addition, we observe that the more the number of bits, the more accurate the estimate. Interestingly, the MSE with 2- or 3-bit quantization is very close to the CRB in the case of no quantization. Hence, it suffices to transmit 2 or 3 bits per sample to achieve the estimation performance close to that of the unquantized approach. Fig. 6(b) also tells us that when the channel is distortional (e.g., $\tilde{P} = 0.2$), the MSE approaches the CRB asymptotically with an increasing N. As we can see, the proposed q-bit quantizer's performance is notably better than that of the q-bit uniform quantizer for both two cases.

C. Detection Performance

Based on the asymptotic statistical properties of the GLRT detector presented in (11), the probability of false alarm can be calculated as

$$P_{FA} = 2Q\left(\sqrt{2\ln\eta}\right), \tag{35}$$

where $Q(\cdot)$ denotes the Q-function of the standard Gaussian tail probability.

The detection probability can be given by

$$P_D = \Phi_{\chi_1'^2(\lambda_q)}(2\ln\eta), \tag{36}$$

where $\Phi_{\chi_n'^2(\lambda_q)}(\cdot)$ denotes the right-tail probability of the non-central Chi-squared distribution with n DOFs and noncentrality parameter λ_q. Fig. 7 depicts the detection probability curves of the q-bit proposed GLRT detector versus the number of sensors for $q = 1, 2$, and 3. As a benchmark, the performance of the unquantized detector is also reported. It is demonstrated that

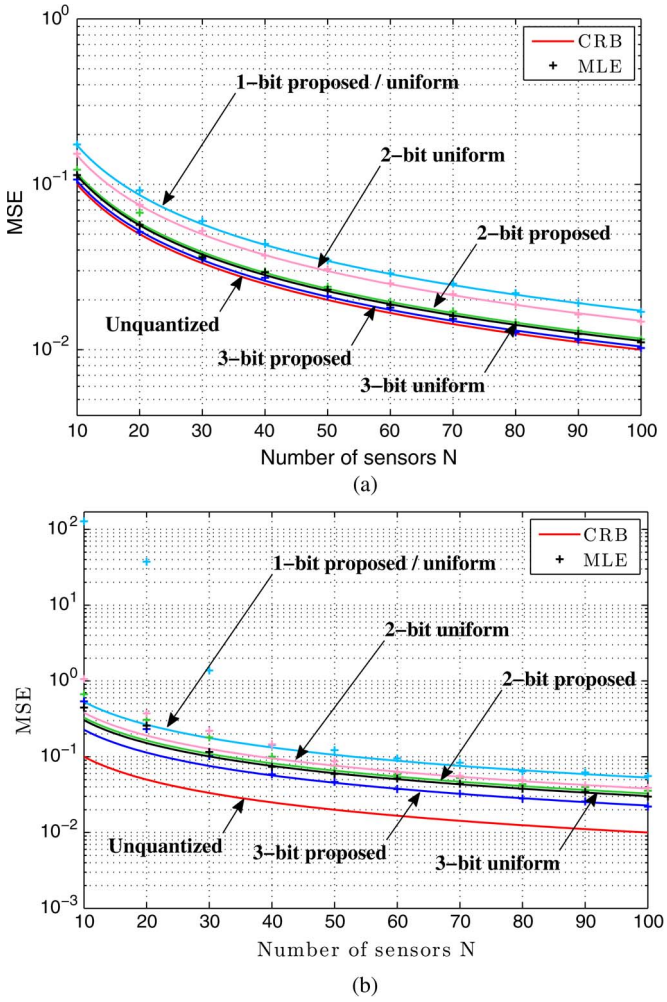

Fig. 6. CRBs and MSEs for the q-bit proposed/uniform schemes; (a) $\tilde{P} = 0$ case; (b) $\tilde{P} = 0.2$ case.

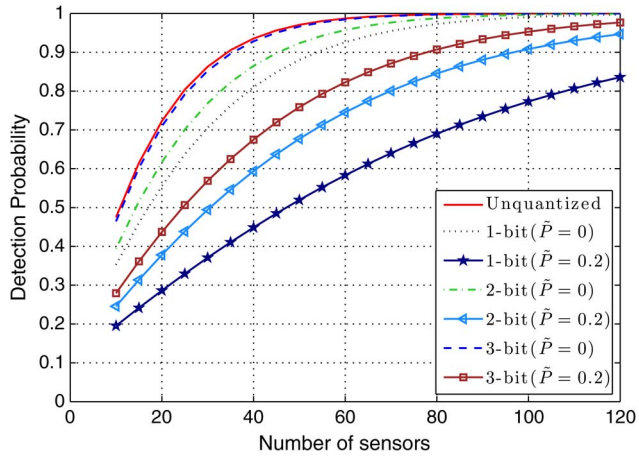

Fig. 7. Performance comparisons of q-bit proposed GLRT detectors for different q and $\tilde{P}$.

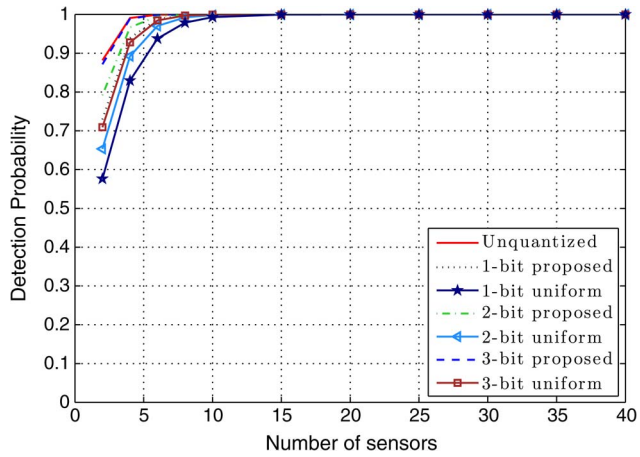

Fig. 8. Performance comparison when $\theta/\sigma^2 = 2$ (i.e., the *weak signal* assumption is removed).

the more the number of quantization bits (or the number of sensors), the better the detection performance. In particular, the detection performance of the 2- or 3-bit detector is very close to that of the unquantized detector without quantization, when the channel is perfect (i.e., $\tilde{P} = 0$). The 3-bit and 2-bit GLRT detector with perfect links achieve the detection probability of about $P_D = 0.86$ and $P_D = 0.82$, respectively, when 30 sensors are employed. The 1-bit counterpart however can only attain a detection probability of approximately 0.7. It reveals again that only 2- or 3-bit quantization is enough for closely achieving the benchmark performance. It is also seen from Fig. 7 that the performance of the quantized GLRT detector is notably degraded in the presence of channel errors (e.g., $\tilde{P} = 0.2$ in this example).

Note that the proposed quantization scheme is proposed under the assumption of weak signal. It is of interest to examine its performance when the assumption is removed. Fig. 8 depicts the performance of the proposed scheme and the uniform quantizer in error-free channels when the signal-to-noise ratio (SNR) is set to $\theta/\sigma^2 = 2$. It is seen that with increasing θ, the detection performance for all schemes significantly improves. Interestingly, the proposed quantization scheme does not fall apart as the SNR increases; rather, the benefit of trying to optimize the quantizer diminishes with growing SNR. Indeed, for larger SNR, there is no significant difference between the proposed quantization scheme and the *ad hoc* uniform quantizer, and their performance approach that of using unquantized samples. This also corroborates that it is the weak signal detection that is most critical, which requires more sophisticated designs for quantization and distributed detection.

Fig. 9 plots the receiver operating characteristics (ROC) curves of the unquantized detector and the GLRT detector for $q = 1, 2$, and 3. Both the analytical expressions (derived in Section IV-A) and MC simulations are used to obtain the ROC curves for the cases of $q = 2$ and 3. The number of independent trials used to calculate the detection probability in each case is 10^5. The MC results for each q are denoted by the same symbol "+" for clarity of exposition in Fig. 9. It can be observed that the analytical results match the MC results pretty well. As we can see, the performance of the proposed q-bit GLRT schemes is better than that of the q-bit uniform schemes. We also observe that the increase in the number of quantization bits leads to a significant gain in the detection performance. Nevertheless, when the number of quantization bits increases to only 3, the quantization loss can be negligible.

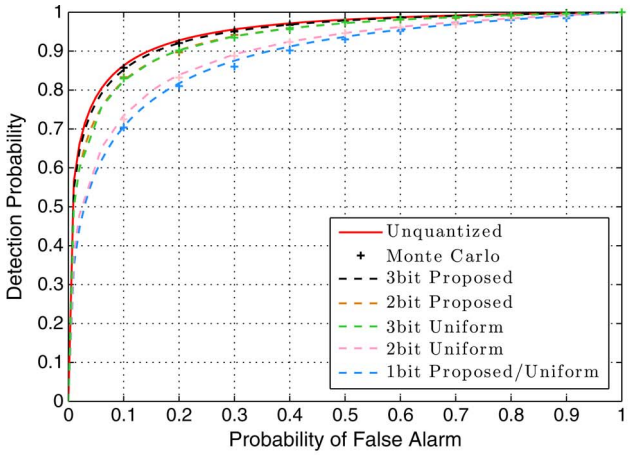

(a)

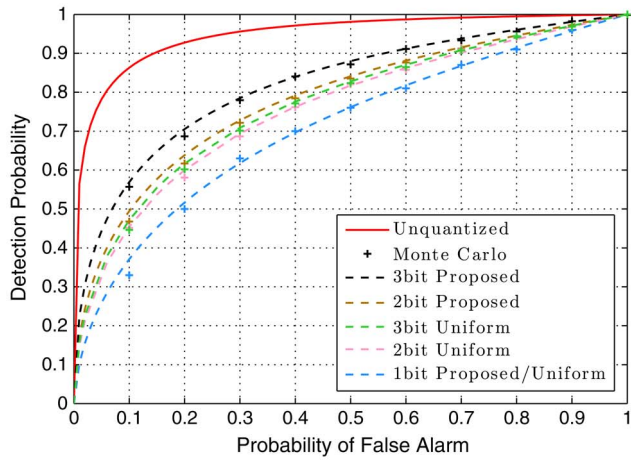

(b)

Fig. 9. ROC curves of q-bit GLRT detectors for different q and $\tilde{P}$, when $N = 30$; (a) $\tilde{P} = 0$ case; (b) $\tilde{P} = 0.2$ case.

D. Mismatch Channels

As shown in (21), *a priori* knowledge of the crossover probability $\tilde{P}$ in the distortion channel is required in the quantizer design. In practice, this crossover probability may be unknown, and needs to be estimated. Denote by $\hat{P}$ the estimated crossover probability. Obviously, there inevitably exists an error in the estimate of the crossover probability. In the following, we examine the effect of the estimation error in the crossover probability on the performance of the proposed GLRT detector. As an example, we consider the case of $q = 2$. Fig. 10 shows the detection probability curves as a function of the number of sensors for different estimated crossover probabilities $\hat{P}$, where the actual crossover probability $\tilde{P}$ is 0.2. Note that the quantization thresholds are obtained by the PSOA for the estimated crossover probability $\hat{P}$. Apparently, there exists mismatch when these thresholds obtained for $\hat{P}$ are applied to the case of $\tilde{P} \neq \hat{P}$. We can observe from Fig. 9 that the error in the crossover probability can produce a non-negligible loss in the detection performance. The more the error, the more the loss in the detection performance.

VI. Conclusion

In this paper, the problem of multilevel quantizer design in WSNs is examined for the distributed detection of a mean parameter corrupted by Gaussian noise. We employ in each sensor a multilevel quantizer determined by a set of quantization thresholds. An asymptotic performance analysis for the GLRT detector is given in terms of probabilities of false alarm and detection. This analysis reveals that the detection performance of the proposed GLRT detector is increasing with the FI. It is shown that the FI is a non-linear and non-convex function of the sets of quantization thresholds. A design criterion for the multilevel quantizers is proposed by maximizing the FI with respect to the quantization thresholds. Because of the non-linearity and non-convexity, we resort to one of evolutionary computation algorithms, i.e., the PSOA, to obtain the quantization thresholds corresponding to the maximal FI. Notice that the PSOA is more suitable than the conventional gradient search approaches for this maximization problem, since the latter is more sensitive to initialization.

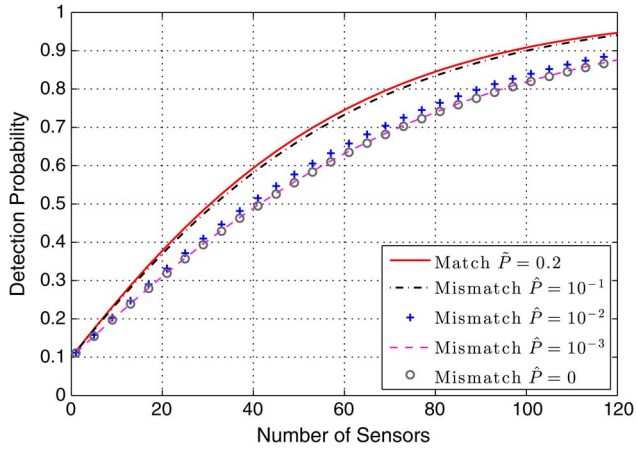

Fig. 10. Performance comparisons of 2-bit GLRT detector for different estimated crossover probabilities $\hat{P}$.

Extensive simulation results are presented, which show that the proposed multi-bit GLRT detector has a notable improvement over the one-bit GLRT detector of [17]. Interestingly, with only 2- or 3-bit quantization, the GLRT detector performs similarly to the unquantized GLRT detector which utilized the original observations without quantization. Hence, it is enough to closely achieve the benchmark performance by using only a small number of quantization bits. Further increase in the number of quantization bits bring in negligible gain in the detection performance, except adding communication burdens and computational complexity.

Appendix A
Proof of (13)

In the light of (9), the natural logarithm of the likelihood function $\tilde{L}_q(\theta)$ is given by

$$\tilde{L}_q(\theta) = \ln L_q(\mathbf{Y};\theta) = \sum_{n=1}^{N}\sum_{i=1}^{2^q} I(\mathbf{y}_n, \mathbf{b}_{n,i}) \ln f_{n,i}, \tag{37}$$

where

$$f_{n,i} = \sum_{j=1}^{2^q} G\left(q, \tilde{P}, D_{n,i,j}\right) P_{w_n}^{n,j}(\theta), \tag{38}$$

with $P_{w_n}^{n,j}(\theta)$ defined in (3). Accordingly, the second-order derivative of $\tilde{L}_q(\theta)$ with respect to θ can be calculated as

$$\frac{\partial^2 \tilde{L}_q(\theta)}{\partial \theta^2} = \sum_{n=1}^{N} \sum_{i=1}^{2^q} I(\mathbf{y}_n, \mathbf{b}_{n,i}) \left[\frac{f''_{n,i}}{f_{n,i}} - \left(\frac{f'_{n,i}}{f_{n,i}} \right)^2 \right], \tag{39}$$

where $f'_{n,i}$ and $f''_{n,i}$ denote the first and second derivatives of $f_{n,i}$ with respect to θ, respectively, i.e.,

$$\begin{aligned} f'_{n,i} &= h_n G\left(q, \tilde{P}, D_{n,i,1}\right) \left[-p_{w_n}(\tau_{n,1} - h_n\theta)\right] \\ &+ h_n G\left(q, \tilde{P}, D_{n,i,2}\right) \left[p_{w_n}(\tau_{n,1} - h_n\theta) - p_{w_n}(\tau_{n,2} - h_n\theta)\right] \\ &+ \cdots + h_n G\left(q, \tilde{P}, D_{n,i,2^q}\right) \left[p_{w_n}(\tau_{n,2^q-1} - h_n\theta)\right], \end{aligned} \tag{40}$$

and

$$\begin{aligned} f''_{n,i} &= h_n^2 G\left(q, \tilde{P}, D_{n,i,1}\right) \left[p'_{w_n}(\tau_{n,1} - h_n\theta)\right] \\ &+ h_n^2 G\left(q, \tilde{P}, D_{n,i,2}\right) \left[p'_{w_n}(\tau_{n,2} - h_n\theta) - p'_{w_n}(\tau_{n,1} - h_n\theta)\right] \\ &+ \cdots + h_n^2 G\left(q, \tilde{P}, D_{n,i,2^q}\right) \left[-p'_{w_n}(\tau_{n,2^q-1} - h_n\theta)\right], \end{aligned} \tag{41}$$

where $p_{w_n}(\cdot)$ denotes the PDF of the observation noise w_n; $p'_{w_n}(\cdot)$ represents the first derivative of $p_{w_n}(\cdot)$ with respect to θ.

Define

$$J(\mathbf{y}_n; \theta) = \sum_{i=1}^{2^q} I(\mathbf{y}_n, \mathbf{b}_{n,i}) \left[\frac{f''_{n,i}}{f_{n,i}} - \left(\frac{f'_{n,i}}{f_{n,i}} \right)^2 \right]. \tag{42}$$

The FI with respect to the parameter θ can be written as

$$\begin{aligned} F_q(\theta) &= -E_{\mathbf{Y}} \left\{ \frac{\partial^2 \tilde{L}_q(\theta)}{\partial \theta^2} \right\} = -\sum_{n=1}^{N} \sum_{i=1}^{2^q} J(\mathbf{y}_n = \mathbf{b}_{n,i}; \theta) f_{n,i} \\ &= -\sum_{n=1}^{N} \sum_{i=1}^{2^q} \left[f''_{n,i} - \frac{\left(f'_{n,i}\right)^2}{f_{n,i}} \right]. \end{aligned} \tag{43}$$

Noting that $\sum_{i=1}^{2^q} G(q, \tilde{P}, D_{n,i,j}) = 1$, we have

$$\begin{aligned} \sum_{i=1}^{2^q} f''_{n,i} = h_n^2 \Big\{ &\left[p'_{w_n}(\tau_{n,1} - h_n\theta)\right] \\ &+ \left[p'_{w_n}(\tau_{n,2} - h_n\theta) - p'_{w_n}(\tau_{n,1} - h_n\theta)\right] \\ &+ \cdots + \left[-p'_{w_n}(\tau_{n,2^q-1} - h_n\theta)\right] \Big\} = 0. \end{aligned} \tag{44}$$

Therefore, the FI is given by

$$F_q(\theta) = \sum_{n=1}^{N} h_n^2 \sum_{i=1}^{2^q} \frac{\left\{ \sum_{j=1}^{2^q} G\left(q, \tilde{P}, D_{n,i,j}\right) \rho_{w_n}^{n,j}(\theta) \right\}^2}{\sum_{j=1}^{2^q} G\left(q, \tilde{P}, D_{n,i,j}\right) P_{w_n}^{n,j}(\theta)} \tag{45}$$

where $\rho_{w_n}^{n,j}(\theta)$ is defined in (14). The proof of (13) is now complete.

ACKNOWLEDGMENT

The authors would like to thank the anonymous reviewers and Associate Editor for their helpful and constructive comments that led to a significant improvement of the manuscript.

REFERENCES

[1] T. Wu and Q. Cheng, "Distributed estimation over fading channels using one-bit quantization," *IEEE Trans. Wireless Commun.*, vol. 8, no. 12, pp. 5779–5784, Dec. 2009.
[2] H. Li and J. Fang, "Distributed adaptive quantization and estimation for wireless sensor networks," *IEEE Signal Process. Lett.*, vol. 14, no. 10, pp. 669–672, Oct. 2007.
[3] H. Chen and P. K. Varshney, "Performance limit for distributed estimation systems with identical one-bit quantizers," *IEEE Trans. Signal Process.*, vol. 58, no. 1, pp. 466–471, Jan. 2010.
[4] E. Masazade, R. Rajagopalan, P. K. Varshney, and C. K. Mohan, "A multiobjective optimization approach to obtain decision thresholds for distributed detection in wireless sensor networks," *IEEE Trans. Syst., Man, Cybern. B, Cybern.*, vol. 40, no. 2, pp. 444–457, Apr. 2010.
[5] J. Fang and H. Li, "Hyperplane-based vector quantization for distributed estimation in wireless sensor networks," *IEEE Trans. Inf. Theory*, vol. 55, no. 12, pp. 5682–5699, Dec. 2009.
[6] S. Kar, H. Chen, and P. K. Varshney, "Optimal identical binary quantizer design for distributed estimation," *IEEE Trans. Signal Process.*, vol. 60, no. 7, pp. 3896–3901, Jul. 2012.
[7] J. Fang and H. Li, "Distributed adaptive quantization for wireless sensor networks: From Delta modulation to maximum likelihood," *IEEE Trans. Signal Process.*, vol. 56, no. 10, pp. 5246–5257, Oct. 2008.
[8] X. Yang and R. Niu, "Channel-aware tracking in multi-hop wireless sensor networks with quantized measurements," *IEEE Trans. Aerosp. Electron. Syst*, vol. 49, no. 4, pp. 2353–2368, Oct. 2013.
[9] D. Li, K. D. Wong, Y. H. Hu, and A. M. Sayeed, "Detection, classification, tracking of targets," *IEEE Signal Process. Mag.*, vol. 19, no. 2, pp. 17–29, Mar. 2002.
[10] J. N. Tsitsiklis, "Decentralized detection," in *Advances in Statistical Signal Processing, Signal Detection*, vol. 2, H. V. Poor and J. B. Thomas, Eds. Greenwich, CT, USA: JAI, Jun. 1993, pp. 573–581.
[11] R. Viswanathan and P. K. Varshney, "Distributed detection with multiple sensors: Part I—Fundamentals," *Proc. IEEE*, vol. 85, no. 1, pp. 54–63, Jan. 1997.
[12] R. S. Blum, S. A. Kassam, and H. V. Poor, "Distributed detection with multiple sensors: Part II—Advanced topics," *Proc. IEEE*, vol. 85, no. 1, pp. 64–79, Jan. 1997.
[13] I. F. Akyildiz, W. Su, Y. Sankarasubramaniam, and E. Cayirci, "A survey on sensor networks," *IEEE Commun. Mag.*, vol. 25, no. 3, pp. 102–114, Aug. 2002.
[14] J.-J. Xiao and Z.-Q. Luo, "Decentralized estimation in an inhomogeneous sensing environment," *IEEE Trans. Inf. Theory*, vol. 51, no. 10, pp. 3564–3575, Oct. 2005.
[15] J. Fang and H. Li, "Distributed estimation of Gauss-Markov random fields with one-bit quantized data," *IEEE Signal Process. Lett.*, vol. 17, no. 5, pp. 449–452, May 2010.
[16] J. Fang and H. Li, "Adaptive distributed estimation of signal power from one-bit quantized data," *IEEE Trans. Aerosp. Electron. Syst.*, vol. 46, no. 4, pp. 1893–1905, Oct. 2010.
[17] J. Fang, Y. Liu, H. Li, and S. Li, "One-bit quantizer design for multisensor GLRT fusion," *IEEE Signal Process. Lett.*, vol. 20, no. 3, pp. 257–260, Mar. 2013.
[18] D. Ciuonzo, G. Papa, G. Romano, P. Salvo Rossi, and P. Willett, "One-Bit decentralized detection with a Rao test for multisensor fusion," *IEEE Signal Process. Lett.*, vol. 20, no. 9, pp. 861–864, Sep. 2013.
[19] V. G. Hansen, "Optimization and performance of multilevel quantization in automatic detectors," *IEEE Trans. Aerosp. Electron. Syst.*, vol. AES-10, no. 2, pp. 274–280, Mar. 1974.
[20] C. W. Helstrom, "Improved multilevel quantization for detection of narrowband signals," *IEEE Trans. Aerosp. Electron. Syst.*, vol. 24, no. 2, pp. 141–147, Mar. 1988.
[21] V. A. Aalo and R. Viswanathan, "Multilevel quantization and fusion scheme for the decentralized detection of an unknown signal," in *Proc. Inst. Elect. Eng.—Radar, Sonar Navigat.*, Aug. 2002, vol. 141, no. 1, pp. 37–44.
[22] M. Huang and S. Dey, "Dynamic quantization for multisensor estimation over bandlimited fading channels," *IEEE Trans. Signal Process.*, vol. 55, no. 9, pp. 4696–4702, Sep. 2007.
[23] A. M. Aziz, "A simple and efficient suboptimal multilevel quantization approach in geographically distributed sensor systems," *Signal Process.*, vol. 88, no. 7, pp. 1698–1714, Jul. 2008.
[24] S. G. Iyengar, R. Niu, and P. K. Varshney, "Fusing dependent decisions for hypothesis testing with heterogeneous sensors," *IEEE Trans. Signal Processing*, vol. 60, no. 9, pp. 4888–4897, Sep. 2012.
[25] D. J. Warren and P. K. Willett, "Optimal decentralized detection for conditionally independent sensors," in *Proc. Am. Control Conf.*, Pittsburgh, PA, USA, Jun. 1989, pp. 1326–1329.

[26] R. Niu and P. K. Varshney, "Joint detection and localization in sensor networks based on local decisions," in *Proc. 40th Asilomar Conf. Signals, Syst. Comput.*, Pacific Grove, CA, USA, Oct. 2006, pp. 525–529.
[27] M. H. Chaudhary and L. Vandendorpe, "Power constrained linear estimation in wireless sensor networks with correlated data and digital modulation," *IEEE Trans. Signal Process.*, vol. 60, no. 2, pp. 570–584, Feb. 2010.
[28] Y. Zhou, C. Huang, T. Jiang, and S. Cui, "Wireless sensor networks and the Internet of things: Optimal estimation with nonuniform quantization and bandwidth allocation," *IEEE Sens. J.*, vol. 13, no. 10, pp. 3568–3574, Oct. 2013.
[29] S. J. Zahabi, A. A. Tadaion, and S. Aissa, "Neyman-Pearson cooperative spectrum sensing for cognitive radio networks with fine quantization at local sensors," *IEEE Trans. Commun.*, vol. 60, no. 6, pp. 1511–1522, Jun. 2012.
[30] R. S. Blum and S. A. Kassam, "Optimum distributed constant false alarm rate detection of weak signals," *J. Acoust. Soc. Am.*, vol. 98, no. 1, pp. 221–229, Jul. 1995.
[31] R. C. Eberhart and Y. Shi, "Comparing inertia weights and constriction factors in particle swarm optimization," in *Proc. Congr. Evol. Comput.*, La Jolla, CA, USA, Nov. 2000, vol. 1, pp. 84–88.
[32] M. Clerc, *Particle Swarm Optimization*, 1st ed. London, U.K.: Wiley, 2006.
[33] S. M. Kay, *Fundamentals of Statistical Signal Processing: Detection Theory*. Saddle River, NJ, USA: Prentice-Hall, 1998.
[34] A. Ribeiro and G. B. Giannakis, "Bandwidth-constrained distributed estimation for wireless sensor networks—Part I: Gaussian PDF," *IEEE Trans. Signal Process.*, vol. 54, no. 3, pp. 1131–1143, Mar. 2006.
[35] D. A. Pierre, *Optimization Theory with Applications*. New York, NY, USA: Wiley, 1969.
[36] J. A. Snyman, *Practical Mathematical Optimization: An Introduction to Basic Optimization Theory and Classical and New Gradient-Based Algorithms*, 1st ed. New York, NY, USA: Springer-Verlag, 2005.
[37] J. Kennedy and R. C. Eberhart, "Particle swarm optimization," in *Proc. IEEE Int. Conf. Neural Netw.*, Perth, WA, Australia, November 1995, vol. 4, pp. 1942–1948.
[38] Y. del Valle, G. K. Venayagamoorthy, S. Mohagheghi, and J. C. Hernandez, "Particle swarm optimization: Basic concepts, variants and applications in power systems," *IEEE Trans. Evol. Comput.*, vol. 12, no. 2, pp. 171–195, Apr. 2008.
[39] A. Ismael, F. Vaz, and L. N. Vicente, "A particle swarm pattern search method for bound constrained global optimization," *J. Global Optim.*, vol. 39, no. 2, pp. 197–219, Oct. 2009.
[40] R. C. Farias, E. Moisan, and J.-M. Brossier, "Optimal asymmetric binary quantization for estimation under symmetrically distributed noise," *IEEE Signal Process. Lett.*, vol. 21, no. 5, pp. 523–526, May 2014.
[41] J. Max, "Quantizing for minimum distortion," *IRE Trans. Inf. Theory*, vol. 6, no. 1, pp. 7–12, Mar. 1960.
[42] S. M. Kay, *Fundamentals of Statistical Signal Processing: Estimation Theory*. Upper Saddle River, NJ, USA: Prentice-Hall, 1993.

Fei Gao received the B.S. degree in communication engineering from the National University of Defense Technology, Changsha, China, in 2007 and the M.S. degree in communication and information system from Harbin Engineering University, Harbin, China, in 2010. He is currently working toward the Ph.D. degree with the College of Information and Communication Engineering, Harbin Engineering University. From September 2012 to April 2014, he was a Visiting Scholar in the Department of Electrical and Computer Engineering, Stevens Institute of Technology, Hoboken, NJ, USA. His current research interests include statistical signal processing, distributed detection, and estimation.

Lili Guo (M'04) received the B.S. degree in automation and the Ph.D. degree from Harbin Engineering University, Harbin, China, in 1982 and 2005, respectively.

Since 1982, he has been with the College of Information and Communication Engineering, Harbin Engineering University, where he became a Professor in 1997. From April 1994 to October 1995, he was a Research Assistant with the Department of Information and Engineering, Tokyo University of Technology. From December 2006 to March 2007, he was a Senior Visiting Scholar with the Department of Information and Engineering, University of Electro-Communications, Tokyo, Japan. His general research interests include highly efficient communication, anti-interference technology, and signal detection and recognition.

Hongbin Li (M'99–SM'08) received the B.S. and M.S. degrees from the University of Electronic Science and Technology of China, Chengdu, China, in 1991 and 1994, respectively, and the Ph.D. degree from the University of Florida, Gainesville, FL, USA, in 1999, all in electrical engineering.

From July 1996 to May 1999, he was a Research Assistant with the Department of Electrical and Computer Engineering, University of Florida. Since July 1999, he has been with the Department of Electrical and Computer Engineering, Stevens Institute of Technology, Hoboken, NJ, USA, where he became a Professor in 2010. He was a Summer Visiting Faculty Member at the Air Force Research Laboratory in the summers of 2003, 2004, and 2009. His general research interests include statistical signal processing, wireless communications, and radars.

Dr. Li has been a member of the IEEE SPS Signal Processing Theory and Methods (2011 to present) Technical Committee (TC) and the IEEE SPS Sensor Array and Multichannel TC (2006–2012). He has been involved in various conference organization activities, including serving as a General Cochair for the Seventh IEEE Sensor Array and Multichannel Signal Processing Workshop held in Hoboken, NJ, USA, on June 17–20, 2012. He is/was an Associate Editor of Signal Processing (Elsevier), the IEEE TRANSACTIONS ON SIGNAL PROCESSING, the IEEE SIGNAL PROCESSING LETTERS, and the IEEE TRANSACTIONS ON WIRELESS COMMUNICATIONS and a Guest Editor of the IEEE JOURNAL OF SELECTED TOPICS IN SIGNAL PROCESSING and EURASIP Journal on Applied Signal Processing. He was a recipient of the Sigma Xi Graduate Research Award from the University of Florida in 1999, the Jess H. Davis Memorial Award for excellence in research in 2001 from Stevens Institute of Technology, the Harvey N. Davis Teaching Award in 2003, the Outstanding Paper Award from the IEEE AFICON Conference in 2011, and the IEEE Jack Neubauer Memorial Award in 2013 from the IEEE Vehicular Technology Society. He is also a member of Tau Beta Pi and Phi Kappa Phi.

Jun Liu (S'11–M'13) received the B.S. degree in mathematics from Wuhan University of Technology, Wuhan, China, in 2006, the M.S. degree in mathematics from the Chinese Academy of Sciences, Beijing, China, in 2009, and the Ph.D. degree in electrical engineering from Xidian University, Xi'an, China, in 2012.

From July 2012 to December 2012, he was a Postdoctoral Research Associate with the Department of Electrical and Computer Engineering, Duke University, Durham, NC, USA. From January 2013 to September 2014, he was a Postdoctoral Research Associate with the Department of Electrical and Computer Engineering, Stevens Institute of Technology, Hoboken, NJ, USA. He is currently with the National Laboratory of Radar Signal Processing, Xidian University, where he is an Associate Professor. His current research interests include statistical signal processing, optimization algorithms, passive sensing, cognitive radar, and multistatic radar.

Jun Fang (M'08) received the B.S. and M.S. degrees from Xidian University, Xi'an, China, in 1998 and 2001, respectively, and the Ph.D. degree from National University of Singapore, Singapore, in 2006, all in electrical engineering.

During 2006, he was a Postdoctoral Research Associate with the Department of Electrical and Computer Engineering, Duke University. From January 2007 to December 2010, he was a Research Associate with the Department of Electrical and Computer Engineering, Stevens Institute of Technology. Since January 2011, he has been with the University of Electronic of Science and Technology of China, Chengdu, China. His current research interests include distributed signal processing, sparse theory and compressed sensing, and Bayesian inference for data analysis.

Dr. Fang is an Associate Technical Editor of the *IEEE Communications Magazine* and an Associate Editor of the IEEE SIGNAL PROCESSING LETTERS. He was a recipient of the IEEE Jack Neubauer Memorial Award in 2013 for the best systems paper published in the IEEE TRANSACTIONS ON VEHICULAR TECHNOLOGY and the Outstanding Paper Award from the IEEE AFICON Conference in 2011.